Presented at the 28th IEEE Photovoltaic Specialists Conference – Anchorage, Alaska, Sep. 15-22, 2000

NEXT-GENERATION, HIGH-EFFICIENCY III-V MULTIJUNCTION SOLAR CELLS

R. R. King, N. H. Karam, J. H. Ermer, M. Haddad, P. Colter, T. Isshiki, H. Yoon, H. L. Cotal, D. E. Joslin,
D. D. Krut, R. Sudharsanan, K. Edmondson, B. T. Cavicchi, and D. R. Lillington
Spectrolab, Inc., 12500 Gladstone Ave., Sylmar, CA 91342

ABSTRACT

Next-generation solar cell approaches such as AlGaInP/GaAs/GaInNAs/Ge 4-junction cells, lattice-mismatched GaInP/GaInAs/Ge, concentrator cells, and improved 3-junction device structures hold the promise of greater efficiency than even today's highly successful multijunction cells. Wide-bandgap tunnel junctions, improved heterointerfaces, and other device structure improvements have recently resulted in several record-efficiency GaInP/GaAs/Ge cell results. Triple-junction (3J) cells grown in this work have demonstrated 29.3% efficiency for space (AM0, 1 sun). Space concentrator 3J cells have efficiency up to 30.0% at low concentration (AM0, 7.6 suns), and terrestrial concentrator cells grown at Spectrolab and processed at NREL have reached 32.3% (AM1.5D, 440 suns).

INTRODUCTION

Monolithic, multijunction III-V solar cells, such as GaInP/GaAs/Ge triple-junction (3J) cells, have given the highest conversion efficiencies of any two-terminal photovoltaic device to date[1-4]. Although quite robust, these are intricate devices, with approximately 20 active semiconductor layers that interact with one another optically, electrically, and via defect diffusion during growth. As high as these efficiencies are, improvements to the device structures shown in Fig. 1 are resulting in still higher efficiencies. Under the space solar spectrum, triple-junction cells grown and fabricated at Spectrolab have demonstrated a record 29.3% efficiency (AM0, 0.1353 W/cm^2, 28°C). Under the concentrator terrestrial spectrum, GaInP/GaAs/Ge triple-junction devices grown at Spectrolab, and metallized and measured at NREL, have a record efficiency of 32.3% (AM1.5D, 44 W/cm^2, 25°C) [4,5]. This paper discusses the device structures that have led to these record-efficiency cells, such as tunnel junctions composed of wide-bandgap semiconductors, and next-generation cell structures that hold the potential for further efficiency increases. These structures include AlGaInP/GaAs/GaInNAs/Ge 4-junction cells[6-9], lattice-mismatched GaInP/GaInAs multijunction cells[10-12], and concentrator solar cells for space[4,13]. The 'flat cell' design has also been developed, with a monolithically integrated bypass diode to markedly simplify packaging, and maintain a uniform thickness across the entire area of the 140-µm (5.5-mil) thick cell[14].

APPROACH

A cross-section of the epitaxial layers that make up the device structure of a Spectrolab GaInP/GaAs/Ge triple-junction solar cell is shown in Fig. 1. The high-efficiency one-sun and concentrator results above benefit from improvements to the cell structures indicated. For example, the top cell window/emitter resistance was decreased while maintaining high blue response; better control over the group-III sublattice ordering and bandgap in the GaInP top cell was achieved, which is critical for current matching; the middle cell window/emitter interface was optimized to reduce recombination and increase V_{oc}, as was the middle cell base/BSF interface; current collection was improved by optimizing the thickness of the middle cell; and recombination in the Ge bottom cell was reduced by passivating and thinning the Ge emitter. Key improvements came from use of wide-bandgap layers in the tunnel junction connecting top and middle cells[15,16], to minimize absorption in these heavily-doped layers with poor minority-carrier lifetime, and from improved crystal structure in the active cell layers.

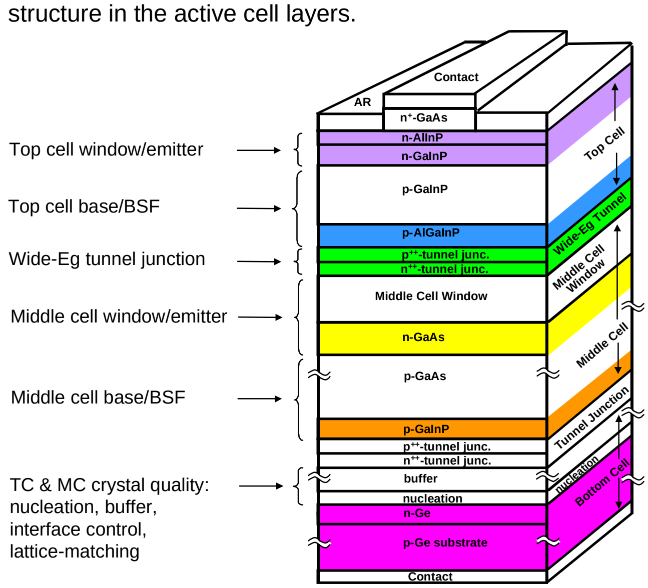

Fig. 1. Cross-section of epitaxial layers in the 3J solar cell,showing improved regions to reach higher efficiencies.

EXPERIMENTAL RESULTS

The crystallinity and morphology is strongly influenced by nucleation conditions and interface control, and was found to be correlated to the cell V_{oc}. For single-junction middle cells, Fig. 2 shows that small values of the full-width half-maximum (FWHM) of x-ray diffraction (XRD) peaks, indicative of a high degree of crystal quality, tend to result in significantly higher open-circuit voltage.

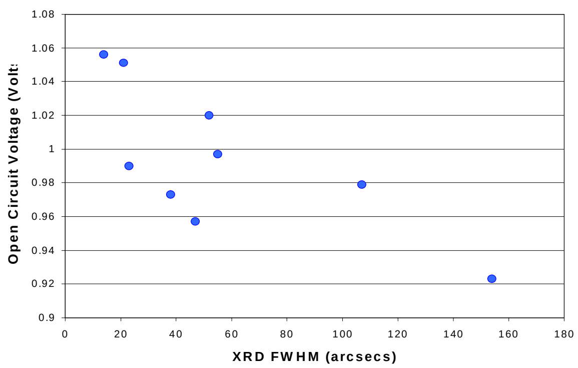

Fig. 2. Open-circuit voltage as a function of full-width half-maximum of x-ray diffraction peaks, for cells grown so that only the middle cell is active.

The dramatically reduced absorption for the p-AlGaAs/n-GaInP wide-bandgap tunnel junction compared to the standard p-GaAs/n-GaAs tunnel junction is illustrated in Fig. 3. Parasitic absorption is reduced due to the shorter wavelength cutoff of the absorption characteristic of the AlGaAs/GaInP tunnel junction, at ~675 nm as opposed to 900 nm for GaAs/GaAs. This effect is magnified by the fact that most of the light with wavelength shorter than 675 nm has already been absorbed by the GaInP top cell by the time it reaches the tunnel junction. In addition, the absorption coefficients for AlGaAs and GaInP are roughly half that of GaAs at around 500 nm. The Burstein-Moss shift has been observed to increase the transmittance of near-bandgap photon energies on these n-type layers, but since this effect is not well quantified for our layers, the Burstein-Moss shift as well as bandgap narrowing effects were not included in the absorption model. The theoretical gain in photogenerated current density J_{ph} by using an AlGaAs/GaInP tunnel junction as opposed to GaAs/GaAs is shown in Fig. 3, obtained by summing the difference between the absorbed J_{ph} curves for the two tunnel junctions, from short to long wavelengths. Experimental data for this gain, obtained by taking the difference between the internal QE measured on cells with AlGaAs/GaInP and GaAs/GaAs tunnel junctions, and integrating this difference across the AM0 spectrum, shows good agreement with theory.

These improvements and others have resulted in the record efficiency light I-V characteristics for a two-terminal solar cell shown in Fig. 4. The V_{oc} of this 3-junction 4.0-cm^2 cell is 2.651 V, due to the reduction of recombination in each subcell through improved interfaces and crystallinity. The J_{sc} is 17.73 mA/cm^2 due in part to the decreased parasitic absorptance of the wide-bandgap tunnel junction, and the efficiency is 29.3% (AM0, 0.1353 W/cm^2, 28°C). Large-area (26.62 cm^2) 3J cells have reached 29.0% AM0 efficiency at Spectrolab. A record 2-junction (2J) cell with 27.2% AM0 efficiency, grown on a Ge substrate, is also shown in Fig. 4. The average efficiency of all 3J cells (>500 cells) in the population of experimental runs in Fig. 5 is 27.7%, so that the average efficiency exceeds the record efficiency of only several months ago. The high-efficiency cell structures used in these record cells are compatible with the high radiation hardness (P/P_o = 0.83 @ 10^{15} e^-/cm^2) typical of 3J GaInP/GaAs/Ge cells[4,17]. Fig. 6 shows the quantum efficiency of each subcell in the record-efficiency 3J cell.

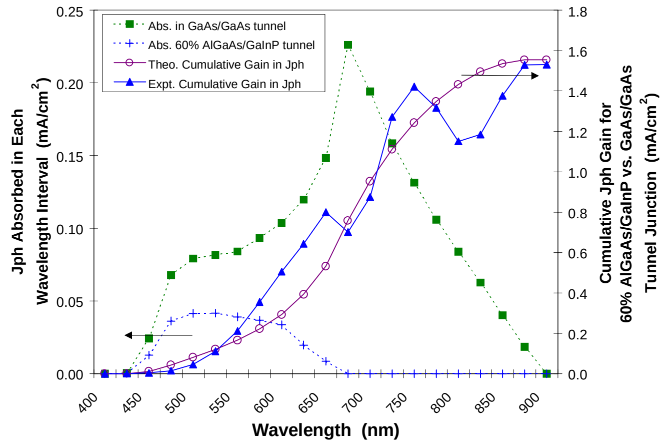

Fig. 3. The photogenerated current density Jph absorbed in a standard GaAs/GaAs tunnel junction and a wide-bandgap AlGaAs/GaInP tunnel junction.

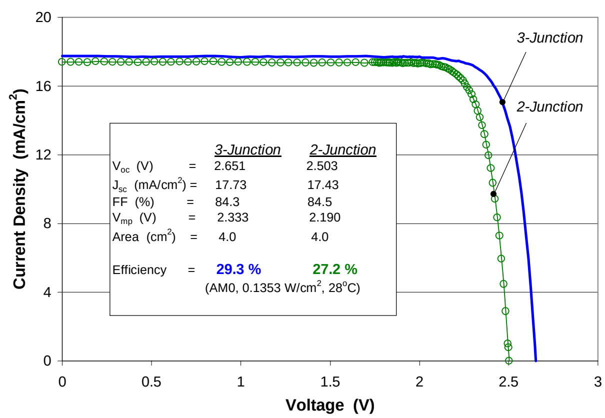

Fig. 4. Light I-V characteristics for record-efficiency 3J and 2J cells under the AM0 spectrum.

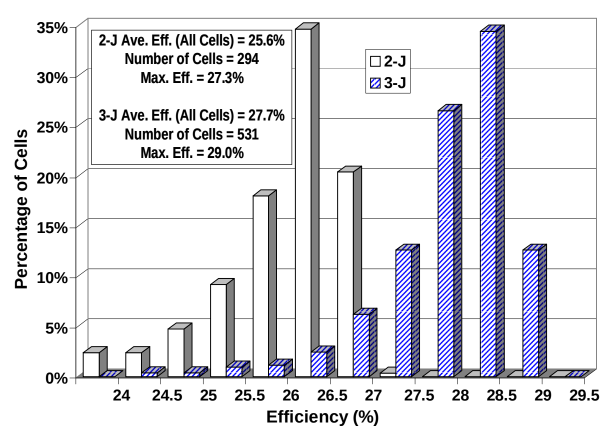

Fig. 5. Distribution of all 531 3J and 294 2J 4.0-cm^2 cells with improved growth process in experimental runs.

Similar cell improvements have resulted in the 32.3% terrestrial concentrator cell described above[4,5], and in 30.0%-efficient space concentrator cells at 7.6 suns (AM0, 1.03 W/cm^2, 25°C) [4]. Fig. 7 shows the light I-V characteristics of this 4.11-cm^2 3J cell at this intensity and at 1.0-sun, showing the higher FF at 7.6 suns.

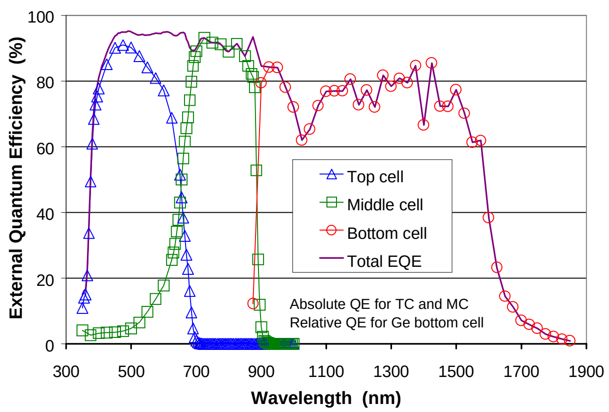

Fig. 6. External quantum efficiency of the top, middle, and Ge bottom subcells in the record efficiency 3J cell.

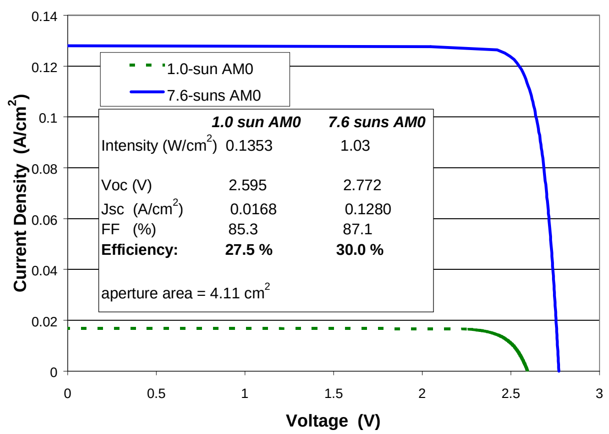

Fig. 7. Concentrator 3J cells measured at 7.6 suns AM0.

Heavily-metallized 3J cells that were current matched to the AM0 spectrum, with 1 cm X 1 cm aperture area, were measured at much higher concentrations using a high-intensity pulsed solar simulator (HIPSS) as shown in Fig. 8. The incident intensity was determined from measured spectral response and integrated, one-sun short-circuit current densities on the top (GaInP) subcell J_T, and the middle subcell J_M . The current through the multijunction stack is determined by the smallest of these current densities, J_{min} . However, by current-matching the cells for a particular spectrum, *e.g.*, by tuning the thickness and bandgap of the GaInP top cell, a J_{sc} of approximately $(J_T + J_M)/2$ should be possible to achieve. An AM0 efficiency of 29% at 20 W/cm^2 was reached by the cell in Fig. 8, using J_{min} (closed circles), but over 30% should be possible by better tuning the current match for AM0 (open circles). Similarly, although this cell was grossly current-mismatched for the AM1.5D spectrum with J_T/J_M = 0.74 for this spectrum, an AM1.5D efficiency of 33.4% at 200 suns is projected for this type of cell upon current matching, consistent with the very high concentrator cell efficiencies measured in [5].

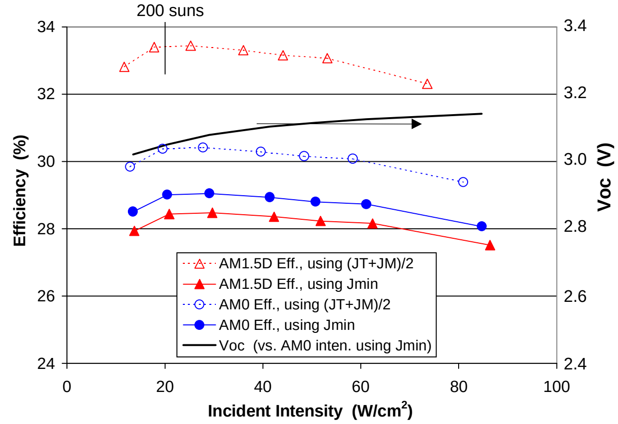

Fig. 8. Measured 3J cell efficiencies (closed symbols) and current-matched projected efficiencies (open symbols) for the AM0 and AM1.5D spectra in the ~100-700 sun range.

The next step beyond optimization of the current triple-junction cell is being taken, with the investigation of the 4-junction (Al)GaInP/GaAs/GaInNAs/Ge cell at Spectrolab under the USAF Dual-Use Science and Technology (DUS&T) program. Growing a 1-eV GaInNAs subcell, lattice-matched to GaAs, between the Ge and GaAs subcells, results in a 4-junction structure that divides the solar spectrum for more efficient energy conversion [6], as shown in Fig. 9. Maximum AM0 efficiencies of 39% are projected to be possible with this technology. Growth of high-quality GaInNAs with long minority-carrier diffusion length, or with small enough background doping to grow a wide intrinsic region for carrier collection in a *pin* device, remains the main technical barrier to this approach[9]. A parallel approach to higher efficiency that is being pursued in the DUS&T program is to tune the bandgap of the subcells in a monolithic 3-junction cell in order to approach the optimum wavelength division of the solar spectrum[10].

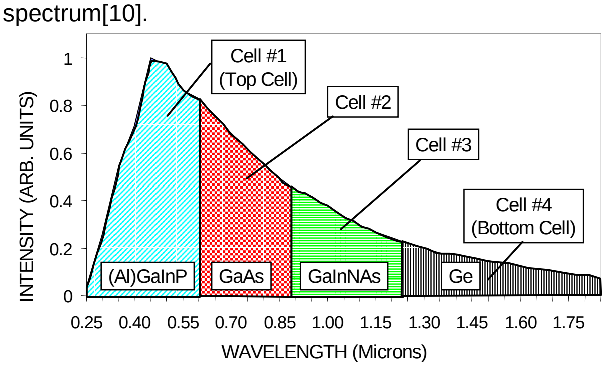

Fig. 9. Division of the AM0 spectrum in a 4-junction AlGaInP/GaAs/GaInNAs/Ge solar cell.

For both the 4-junction cell with GaInNAs and the lattice-mismatched GaInP/GaInAs/Ge cell approaches, as well as the more conventional lattice-matched GaInP/GaAs/Ge 3-junction cell, modeling indicates that the highest efficiencies are possible for higher top-cell bandgaps. This can be achieved by using group-III sublattice disordering in GaInP, alloying with Al to form AlGaInP-base top cells, or a combination of the two. Fig. 10 plots data from a study of the effect of Al concentration, substrate orientation, and Zn doping level on sublattice disorder and bandgap in AlGaInP top cells. Increasing the Ge substrate miscut angle from (100) to induce sublattice disorder was successful in changing the bandgap E_g of GaInP over a range of ~0.07 eV, as measured both by photoluminescence (PL), and by extraction from the bandedge of QE measurements. With the addition of 10% Al, substrate misorientation varied the bandgap of $Al_{0.1}Ga_{0.4}In_{0.5}P$ over a range of ~0.05 eV, reaching values up to 2.0 eV for some samples as measured by PL. The V_{oc} of the GaInP cells increased with bandgap, but by less than 1 mV for each meV change in E_g. Higher V_{oc} values were observed for the medium-doped $Al_{0.1}Ga_{0.4}In_{0.5}P$ cells at low miscut angles than for $Ga_{0.5}In_{0.5}P$, but the AlGaInP V_{oc} dropped off with increasing E_g at the highest miscut angle. J_{sc} of both the GaInP and AlGaInP cells decreased at the expected rate as the bandgap of each material increased with miscut angle. However, the J_{sc} of the AlGaInP cells was offset by about 2 mA/cm^2 lower than the GaInP, probably due to lower base lifetime due to some oxygen contamination in the AlGaInP, or due to imperfect passivation at the back surface of these wide-bandgap cell bases.

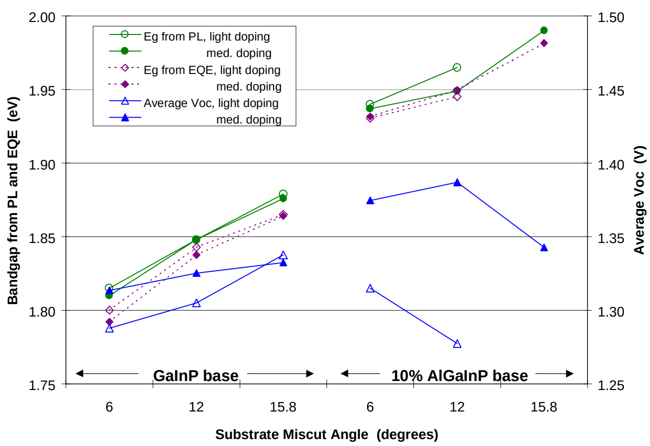

Fig. 10. Bandgap and V_{oc} of GaInP and AlGaInP top cells, as a function of substrate miscut angle.

SUMMARY

Experiments to improve GaInP/GaAs/Ge multijunction cell structures, such as wide-bandgap tunnel junctions and improved crystallinity, have recently resulted in record-efficiency cell results. Triple-junction (3J) cells grown in this work have demonstrated 29.3% efficiency for space (AM0, 1 sun). Space concentrator 3J cells have efficiency up to 30.0% at low concentration (AM0, 7.6 suns), and terrestrial concentrator cells grown at Spectrolab and processed at NREL have 32.3% (AM1.5D, 440 suns). Work on next-generation cell approaches, such as AlGaInP/GaAs/GaInNAs/Ge 4-junction cells and lattice-mismatched GaInP/GaInAs/Ge 3J cells, is expected to increase these efficiencies still further.

ACKNOWLEDGMENTS

The authors would like to thank Clay Mayberry and Kitt Reinhardt of the Air Force Research Laboratory, Dean Marvin of the Aerospace Corporation, Mark Takahashi, Raed Sherif, and the entire multijunction solar cell team at Spectrolab. This work was supported in part by the Air Force Research Laboratory (AFRL/VS) under DUS&T contract # F29601-98-2-0207, and by Hughes Spectrolab.

REFERENCES

1. J. M. Olson, S. R. Kurtz, A. E. Kibbler, P. Faine, "A 27.3% Efficient $Ga_{0.5}In_{0.5}P$/GaAs Tandem Solar Cell," *Appl. Phys. Lett.* **56**, p.623 (1990).
2. T. Takamoto, M Yamaguchi, S. J. Taylor, E. Ikeda, T. Agui, and H. Kurita, "High-Efficiency Radiation Resistant InGaP/GaAs Tandem Solar Cells," *Proc. 26th IEEE Photovoltaic Specialists Conf. (PVSC)* (1997), p. 887.
3. N. H. Karam, R. R. King, B. T. Cavicchi, D. D. Krut, J. H. Ermer, M. Haddad, L. Cai, D. E. Joslin, M. Takahashi, J. W. Eldredge, W. T. Nishikawa, D. R. Lillington, B. M. Keyes, and R. K. Ahrenkiel, *IEEE Trans. on Electron Devices* **46**, p.2116 (1999).
4. N. H. Karam, R. R. King, M. Haddad, J. H. Ermer, H. Yoon, H. L. Cotal, R. Sudharsanan, J. W. Eldredge, K. Edmondson, D, E. Joslin, D. D. Krut, M. Takahashi, W. Nishikawa, M. Gillanders, J. Granata, P. Hebert, B. T. Cavicchi, and D. R. Lillington, "Recent Developments in High-Efficiency $Ga_{0.5}In_{0.5}P$/GaAs/Ge Dual- and Triple-Junction Solar Cells: Steps to Next-Generation PV Cells," to be publ. *Solar Energy Materials and Solar Cells*, 2000.
5. H. L. Cotal, D. R. Lillington, J. H. Ermer, R. R. King, N. H. Karam, S. R. Kurtz, D. J. Friedman, J. M. Olson, J. S. Ward, A. Duda, K. A. Emery, T. Moriarty, "Triple-Junction Solar Cell Efficiencies Above 32%: The Promise and Challenges of Their Application in High-Concentration-Ratio PV Systems," to be publ. *Proc. 28th IEEE PVSC* (2000).
6. S. R. Kurtz, D. Myers, J. M. Olson, "Projected Performance of Three- and Four-Junction Devices Using GaAs and GaInP," *Proc. 26th IEEE PVSC* (1997), p.875.
7. D.J. Friedman et al., "1-eV GaInNAs Solar Cells for Ultrahigh-Efficiency Multijunction Devices," *2nd World Conf. on PV Energy Conv.* (1998).
8. Steven Kurtz et al., "InGaAsN Solar Cells with 1.0 eV Band Gap, Lattice Matched to GaAs," *Appl. Phys. Lett.*, Feb. 1999, p. 729.
9. Sarah Kurtz et al., "Modeling of Electron Diffusion Length in GaInAsN Solar Cells," to be publ. *Proc. 28th IEEE PVSC* (2000).
10. R. R. King, M. Haddad, T. Isshiki, P. Colter, J. Ermer, H. Yoon, D. E. Joslin, and N. H. Karam, "Metamorphic GaInP/GaInAs/Ge," to be publ. *Proc. 28th IEEE PVSC* (2000).
11. F. Dimroth, P. Lanyi, U. Schubert, and A. W. Bett, "MOVPE Grown $Ga_{1-x}In_xAs$ Solar Cells for GaInP/GaInAs Tandem Applications," *J. Electronic Materials* **29**, p.42 (2000).
12. F. Dimroth, U. Schubert, and A. W. Bett, "25.5% Efficient $Ga_{0.35}In_{0.65}P/Ga_{0.83}In_{0.17}As$ Tandem Solar Cells Grown on GaAs Substrates," *IEEE Electron Device Lett.* **21**, p.209 (2000).
13. D. D. Krut, G. S. Glenn, B. Bailor, M. Takahashi, R. A. Sherif, D. R. Lillington, N. H. Karam, U. Ortabasi, "Wide Acceptance Angle, Non-Imaging, Triple-Junction Based, 10X Composite Space Concentrator," to be publ. *Proc. 28th IEEE PVSC* (2000).
14. J. E. Granata, J. H. Ermer, P. Hebert, M. Haddad, R. R. King, D. D. Krut, J. Lovelady, M. S. Gillanders, N. H. Karam, B. T. Cavicchi, "Triple-Junction $GaInP_2$/GaAs/Ge Solar Cells – Production Status, Qualification Results, and Operational Benefits," to be publ. *Proc. 28th IEEE PVSC* (2000).
15. D. Jung, C. Parker, J. Ramdani, and S. Bedair, "AlGaAs/ GaInP heterojunction tunnel diode for cascade solar cell application," *J. Appl. Phys.*, Vol. 74, No. 3, p. 2090, 1993.
16. F. Dimroth et al., "High C-Doping of MOVPE Grown Thin $Al_xGa_{1-x}As$ Layers for AlGaAs/GaAs Interband Tunneling Devices," *J. Elec. Matl.*, vol. 29, Jan. 2000, p.47.
17. H. L. Cotal, R. R. King, M. Haddad, J. H. Ermer, N. H. Karam, D. D. Krut, D. E. Joslin, M. Takahashi, B. T. Cavicchi, "The Effects of Electron Irradiation on Triple-Junction $Ga_{0.5}In_{0.5}P$/GaAs/Ge Solar Cells," to be published in *Proc. 28th IEEE PVSC* (2000).